Neuroscience Research 156 (2020) 58–65

Contents lists available at ScienceDirect

Neuroscience Research

journal homepage: www.elsevier.com/locate/neures

Neurotransmission through dopamine D1 receptors is required for aversive memory formation and Arc activation in the cerebral cortex

Nae Saito[a,b], Kazuki Tainaka[c], Tom Macpherson[d], Takatoshi Hikida[d], Shun Yamaguchi[e,f], Toshikuni Sasaoka[a,*]

[a] Department of Comparative and Experimental Medicine, Brain Research Institute, Niigata University, 1-757 Asahimachidori, Chuo-ku, Niigata, 951-8585, Japan
[b] Department of Molecular and Cellular Medicine, Graduate School of Medical and Dental Sciences, Niigata University, 1-757 Asahimachidori, Chuo-ku, Niigata, 951-8585, Japan
[c] Department of System Pathology for Neurological Disorders, Brain Research Institute, Niigata University, 1-757 Asahimachidori, Chuo-ku, Niigata, 951-8585, Japan
[d] Laboratory for Advanced Brain Functions, Institute for Protein Research, Osaka University, 3-2 Yamadaoka, Suita, Osaka, 565-0871, Japan
[e] Department of Morphological Neuroscience, Graduate School of Medicine, Gifu University, 1-1 Yanagido, Gifu City, Gifu, 501-1194, Japan
[f] Center for Highly Advanced Integration of Nano and Life Sciences, Gifu University, 1-1 Yanagido, Gifu City, Gifu, 501-1194, Japan

ARTICLE INFO

Article history:
Received 27 September 2019
Received in revised form 22 April 2020
Accepted 24 April 2020
Available online 5 May 2020

Keywords:
Dopamine D1 receptor
Aversive memory
Arc
Arg3.1
Venus
Three-dimensional imaging

ABSTRACT

Dopaminergic neurotransmission is considered to play an important role not only in reward-based learning, but also in aversive learning. Here, we investigated the role of dopaminergic neurotransmission via dopamine D1 receptors (D1Rs) in aversive memory formation in a passive avoidance test using D1R knockdown (KD) mice, in which the expression of D1Rs can conditionally and reversibly be controlled by doxycycline (Dox) treatment. We also performed whole-brain imaging after aversive footshock stimulation in activity-regulated cytoskeleton protein (Arc)-dVenus D1RKD mice, which were crossbred from Arc-dVenus transgenic mice and D1RKD mice, to examine the distribution of Arc-controlled dVenus expression in the hippocampus and cerebral cortex during aversive memory formation. Knockdown of D1R expression following Dox treatment resulted in impaired performance in the passive avoidance test and was associated with a decrease in dVenus expression in the cerebral cortex (visual, somatosensory, and motor cortices), but not the hippocampus, compared with control mice without Dox treatment. These findings indicate that D1R-mediated dopaminergic transmission is critical for aversive memory formation, specifically by influencing Arc expression in the cerebral cortex.

© 2020 Published by Elsevier B.V.

1. Introduction

Dopamine transmission is involved in both reward learning and aversive memory formation (Schultz, 2019). Specifically, the D1 dopamine receptor (D1R) or D1-like receptor activity has been reported to be involved in hippocampal CA1 synaptic plasticity and long-term memory related to aversive learning tasks (Lammel et al., 2011, 2012; Menegas et al., 2015; Broussard et al., 2016; Menegas et al., 2018; Weele et al., 2019). D1Rs are also involved in induction of the activity-regulated cytoskeleton protein (Arc, also known as Arg 3.1), which is an immediate-early gene (IEG) in the hippocampal CA1 region required for the transition from early- to late-phase long-term potentiation (Granado et al., 2008). As such, the expression of Arc has been utilized to identify activated neurons during memory formation (Vazdarjanova et al., 2006; Mastwal et al., 2016; Okuno et al., 2018). Arc has several advantages over other IEGs as a marker of neuronal activity. For instance, unlike IEGs that are broadly expressed in many cell types, Arc induction is specific to behavioral tasks, and occurs only in the hippocampus and cerebral cortex (Vazdarjanova et al., 2006; Mastwal et al., 2016). Furthermore, Arc interacts with excitatory postsynaptic receptors (e.g., AMPA receptors) and adaptors (e.g., clathrin adaptor protein 2), thereby having a more direct effect in regulating synaptic functions (Chowdhury et al., 2006; Zhang et al., 2015). The developmental emergence of activity-dependent Arc expression relies on dopaminergic transmission; consequently, frontal dopamine circuits require functional Arc to exert their activities (Mastwal et al.,

Abbreviations: Arc, activity-regulated cytoskeleton protein; D1R, dopamine D1 receptor; D1RKD, dopamine D1 receptor knockdown; Dox, doxycycline; IEG, immediate early gene; LSF, light sheet fluorescence.

* Corresponding author.
E-mail address: sasaoka@bri.niigata-u.ac.jp (T. Sasaoka).

https://doi.org/10.1016/j.neures.2020.04.006
0168-0102/© 2020 Published by Elsevier B.V.

2016). Therefore, specific Arc expression patterns can serve as a marker of the contribution of D1R-mediated dopaminergic transmission in behavioral task-induced neural signals.

In the present study, to analyze Arc signals, we used Arc-dVenus mice, which demonstrate high expression of a promoter-destabilized enhanced protein construct in Arc-expressing cells (Eguchi and Yamaguchi, 2009). Further, we previously generated D1R knockdown (D1RKD) mice in which D1Rs can be conditionally and reversibly regulated by doxycycline (Dox) treatment (Chiken et al., 2015; Okubo et al., 2018). Herein, we crossed D1RKD mice with Arc-dVenus mice to generate Arc-dVenus D1RKD mice that allow for the investigation of the involvement of D1R-mediated neural transmission in aversive memory formation and Arc expression. Recently, several imaging systems have been developed that enable comprehensive analysis of the whole brain, such as Clear, Unobstructed Brain/Body Imaging Cocktails and Computational analysis (CUBIC) and ClearMap (Susaki et al., 2014; Renier et al., 2016). Therefore, we performed whole-brain imaging according to the updated CUBIC protocol (Tainaka et al., 2018) and analyzed the distribution of the expression of the fluorescent protein dVenus under the control of the *Arc* gene with a light sheet fluorescence (LSF) microscope.

2. Material and methods

2.1. Mice

C57BL/6 mice were purchased from CLEA Japan (Tokyo, Japan). The generation of D1R knockdown (KD) mice (D1R homozygous knockout/Tet/Off system-based compound-transgenic mice) followed previously published protocols (Chiken et al., 2015; Okubo et al., 2018). In addition, conditional and reversible Arc-dVenus D1RKD mice were generated by crossing D1RKD mice with Arc-dVenus transgenic mice, which were gifted by Prof. Yamaguchi at Gifu University (Eguchi and Yamaguchi, 2009), according to previously published methods (Chiken et al., 2015; Okubo et al., 2018). Only male mice were used in the present study.

Mice were maintained under a 12-h light/dark cycle (lights on at 7:00 AM), with *ad libitum* access to food and water in specific-pathogen-free conditions. All experiments were performed in accordance with the guidelines of the National Institutes of Health, and the Ministry of Education, Culture, Sports, Science and Technology (MEXT) of Japan and were approved by the Institutional Animal Care and Use Committee of Niigata University.

2.2. Grouping and doxycycline (Dox) treatment

In D1RKD mice and Arc-dVenus D1RKD mice, 2.0 mg/mL doxycycline (Dox; Sigma Aldrich, St. Louis, MO, USA) was used to knock down D1R expression, as previously described (Chiken et al., 2015; Okubo et al., 2018). For mice treated with Dox, Dox was administered via drinking water containing 5% sucrose, for four weeks prior to behavioral tests and until the completion of the learning session during the first phase of the experiment (see Section 2.3 and Fig. 1A), after which all mice received drinking water without Dox for the remainder of the experiment. Mice that were not treated with Dox received Dox-free water for the entire duration of the experiment. In the passive avoidance (PA) test, D1RKD mice were assigned to D1RKD Dox (-) and D1RKD Dox (+) groups with eight mice per group; eight wild-type (WT) mice were used as the control group. In the pain sensitivity assessment, D1RKD mice were assigned to D1RKD Dox (+) and D1RKD Dox (-) groups with six and five mice per group respectively; four WT mice were used as the control group. Arc-dVenus D1RKD mice were assigned to the following four groups: D1RKD Dox (−) Stimulation (−) (n = 3), D1RKD Dox (+) Stimulation (−) (n = 4), D1RKD Dox (−) Stimulation (+) (n = 4), and D1RKD Dox (+) Stimulation (+) (n = 5). Stimulation referred to whether or not the mice received an aversive electric footshock in the PA test and the pain sensitivity assessment (see Sections 2.3–2.5).

2.3. PA test

A step-through-type apparatus, comprising light and dark compartments separated by a removable door, was used for the PA test (O'Hara & Co., Tokyo, Japan). The task involved a learning session and a memory-retention test session. In the former, each mouse was placed in the light compartment on day one. The separating door was removed 30 s later, allowing the subject to enter the dark compartment. At 3 s post-entry, the mouse received a 2 s 0.3-mA electric footshock through the floor grid. Following the completion of this learning session D1RKD Dox (+) mice were removed from Dox administration for the remainder of the experiment. Memory-retention test sessions were then conducted on days 2, 4, 8, and 15. For these sessions, each mouse was placed in the light compartment, and the door to the dark compartment was opened 30 s later. The time required for the subjects to enter the dark compartment was then recorded; if mice did not enter after 300 s, the session was ended. Mice were allowed to acclimate to the testing room for 30 min before testing. See Fig. 1A for a schematic of the experiment.

2.4. Pain sensitivity assessment

The pain sensitivity assessment was performed using the same device as described for the PA test. However, here each mouse was placed in the light compartment and the removable door was left open, allowing the mouse to enter the dark compartment at will. At 3 s post-entry, the mouse received a 2 s 0.3-mA electric footshock, after which the time required for the mouse to return to the light compartment was recorded.

2.5. Treatment prior to imaging

Arc-dVenus D1RKD mice were housed in constant darkness for 3 d. Footshock stimulation was performed in a dark room (10 lx) to avoid visual effects, and was carried out in the same step-through-type apparatus as described for the PA test. Specifically, each mouse received a 2 s 0.3-mA electric footshock. Following footshock stimulation, mice were kept in the dark for 5 h before brain sample collection.

2.6. Clearing protocol

Arc-dVenus D1RKD mice were anesthetized with a mixture of medetomidine hydrochloride (0.75 mg/kg body weight [BW]), midazolam (4 mg/kg BW), and butorphanol tartrate (5 mg/kg BW). The mice were then perfused with phosphate buffered saline (PBS, pH 7.4) and 4% paraformaldehyde in PBS through the left ventricle. The brains were removed, post-fixed overnight in 4% paraformaldehyde in PBS at 4 °C, and stored in PBS. The brains were made transparent for imaging according to the updated CUBIC method (Tainaka et al., 2018). For 4–5 d, the brains were immersed in CUBIC-L [10/10 wt% chemical cocktail of *N*-butyldiethanolamine (Tokyo Chemical Industry, B0725) and Triton X-100 (Nacalai Tesque, 12967-45)] and shaken (80–100 rpm) at 37 °C. The brains were then washed three times with PBS at room temperature for 30 min, then stained for 3 d at room temperature with RedDot™2 (1:100, Biotium Inc., #40061) in PBS containing 0.5 M NaCl. After staining, the brains were washed in PBS and shaken gently in 1:1 diluted CUBIC-R [45/30 wt% chemical cocktail of 45 wt% antipyrine

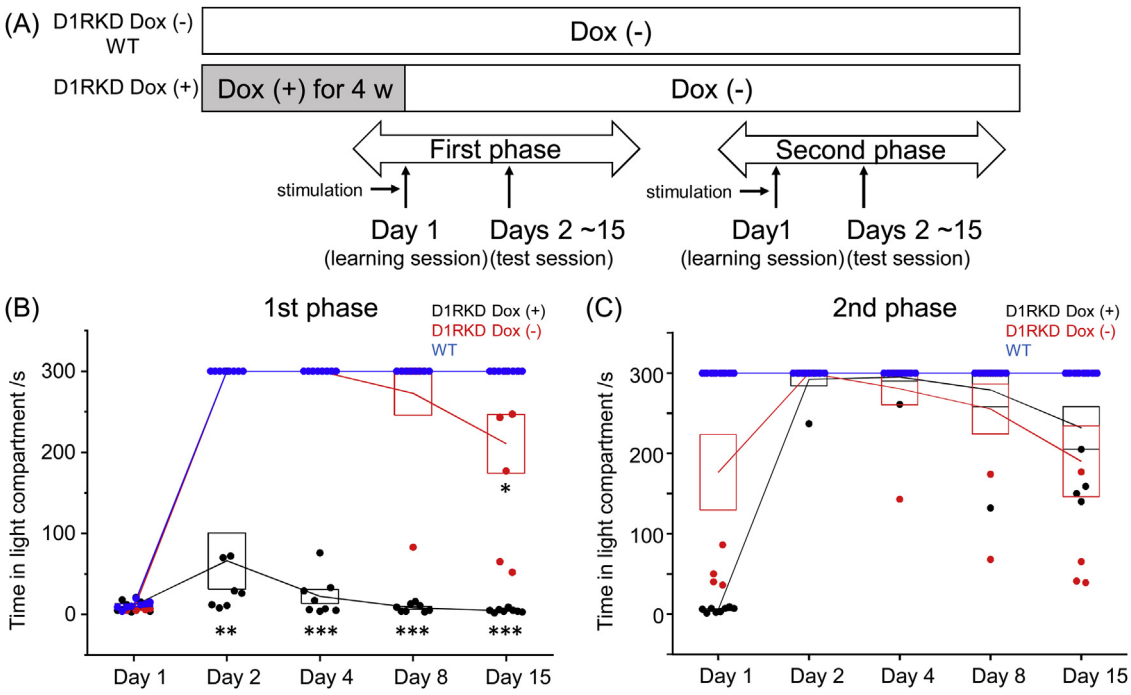

Fig. 1. Passive avoidance test. (A) Experimental schedule. In the D1RKD Dox (+) group, Dox (2 mg/mL) was administered for 4 weeks prior to the commencement of the experiment and until after the completion of the learning session on Day 1 during the first phase of the passive avoidance test, with mice provided drinking water without Dox thereafter. The D1RKD Dox (-) and wild-type (WT) groups were always given only Dox-free water. The learning session on day 1 and test sessions on days 2, 4, 8, and 15 were conducted for both phases in all three groups.
(B) In the first phase, experimenters recorded the latency to enter the dark compartment (or duration remaining in the light compartment) for all three groups during the learning session. *p < 0.05; **p < 0.01; ***p < 0.001. (C) In the second phase, after D1R expression was restored in D1RKD Dox(+) mice, the latency to enter the dark compartment was again recorded for all three groups.

(Tokyo Chemical Industry, D1876) and nicotinamide (Tokyo Chemical Industry, N0078), pH 10 adjusted by *N*-butyldiethanolamine] at room temperature for 6 h, and then shaken gently in CUBIC-R at room temperature overnight. Subsequently, the brains were immersed in new CUBIC-R and again gently shaken at room temperature for at least 6 h.

2.7. Imaging and analysis

Fluorescent images were acquired with custom-built LSF microscopes (MVX10-LS, Olympus) and a 0.63× objective lens (numerical aperture = 0.15, working distance =87 mm) with 1–1.6× digital zoom. The LSF microscope was equipped with lasers emitting at 488 nm and 637 nm. The objective lens accompanied stage movement in the axial direction to avoid defocusing. During image acquisition, refractive index (RI)-matched samples were immersed in a mixture (RI = 1.525) of silicon oil HIVAC-F4 (RI = 1.555, Shin-Etsu Chemical Co., Ltd.) and mineral oil (RI = 1.467, M8410, Sigma Aldrich). Images were collected by scanning samples in the z-direction with a step size of 10 μm. Fluorescent signals were visualized using a laser of appropriate wavelength with sequential shifting of light sheet focal positions. The thinnest focal point of the LSF microscope was horizontally scanned six times per plane to reduce defocusing from the beam's Gaussian shape. Scanning was performed from either side of the illumination arm. Images of identical horizontal positions (dVenus, bandpass emission filter: 495–540 nm; autofluorescence at 488 nm, bandpass emission filter: 600–690 nm; and RedDot^{TM}2 at 637 nm, bandpass emission filter: 660–750 nm) were merged using customized image software (MVX10-MG-SW version 1.1.3, Olympus). To remove autofluorescence signals in the finalized dVenus images, autofluorescence images were subtracted from the dVenus images in Fiji software. Since hippocampal regions displayed comparable dVenus signal intensities regardless of experimental conditions, the average signal intensity values for the hippocampus, calculated using Fiji software, were used to normalize data from individual Arc-dVenus D1RKD mice. Further, considering that brains swell in response to the clearing process, and that the size of the swollen brain differed between experimental groups, the brain size was calculated and normalized using the ratio of the size. Acquired brain images were overlapped via an automatic transformation algorithm (Tainaka et al., 2018) for quantitative comparisons. Reconstitution and analysis of volume-rendered images were conducted in Imaris (version 8.1.2, Bitplane). Using Imaris, a region where the fluorescence intensity of dVenus higher than a certain threshold was found in the normalized brain was set as a measurement region. The number of voxels in the region exhibiting a fluorescence intensity higher than that threshold was calculated. The sum of the number of voxels was converted to the signal volume of the brain region where Arc was activated by footshock stimulation. The dVenus signal was overlaid with the RedDot^{TM}2 signal and the cortical layers were identified depending on the arrangement of neuronal nuclei staining. The areas of cerebral cortex and hippocampus were identified by referring to the Allen Brain Atlas (http://mouse.brain-map.org/).

2.8. Statistical analysis

All data were analyzed in Origin 2019b (OriginLab, Northampton, MA, USA). Data from the PA test and the pain sensitivity assessment were analyzed using Mann-Whitney tests. Normality was evaluated with the Shapiro test, and homogeneity of variance was evaluated with F-tests. Student's *t*-test was used for comparison of imaging data between groups if they met assumptions of normality and homogeneity of variance, whereas Welch's *t*-test was applied if the data were normally distributed but had unequal variance. Significance was judged at $p < 0.05$.

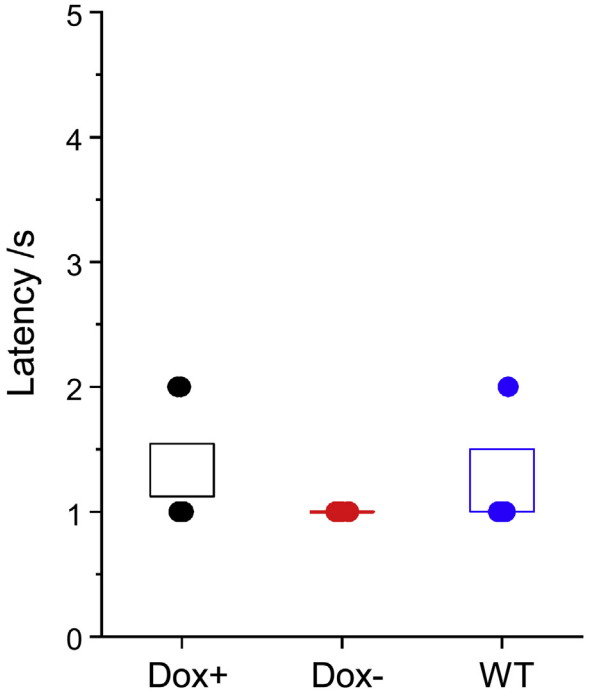

Fig. 2. Pain sensitivity assessment. In the D1RKD Dox (+) group, Dox (2 mg/mL) was administered for 4 weeks prior to commencing the experiment. D1RKD Dox (-) and wild-type (WT) groups were provided Dox-free water. Following elimination of D1R expression in D1RKD Dox (+) mice, the latency for the mouse to return to the light compartment following an electric footshock in the dark compartment was recorded for all three groups.

3. Results

3.1. PA test and pain sensitivity assessment

The first test phase (Fig. 1A) examined the effects of D1R inhibition on a passive avoidance test. While all mice did not significantly differ in the time taken to enter the dark compartment during the learning session (Day 1), D1RKD Dox (+) mice entered the dark compartment significantly quicker than D1RKD Dox (−) or WT mice during all post-conditioning test sessions (Days 2–15) ($p < 0.01$) (Fig. 1B). Indeed, all WT mice avoided the dark compartment until the session ended (300 s) throughout all post-conditioning test sessions (Days 2–15), while D1RKD Dox (−) mice only began to enter the dark compartment before the maximum test time on day 8, with a significant decreased latency to enter by day 15 ($p < 0.05$) (Fig. 1B).

The second test phase (Fig. 1A) examined the effects of recovery of D1R expression on a passive avoidance test. Following footshock conditioning in the dark compartment during the learning session on Day 1, D1RKD Dox (+) mice showed a significantly increased latency to enter the dark compartment on day 2 that was equivalent to WT and D1RKD Dox (−) mice. Furthermore, D1RKD Dox (+) mice in this second phase showed a similar phenotype to the performance of D1RKD Dox (−) mice during both the first and second phases, with a gradual decrease in the latency to enter the dark compartment beginning on Day 8 and becoming more pronounced by Day 15 (Fig. 1C).

The pain sensitivity assessment revealed no significant difference between D1RKD Dox (+) and D1RKD Dox (−) mice in the latency to return to the light compartment compared to that of WT mice, with all mice returning to the light compartment within 2 s: D1RKD Dox (+) mice, 1.3 ± 0.2 s; D1RKD Dox (−) mice, 1.0 ± 0.0 s; WT mice, 1.3 ± 0.3 s (Fig. 2).

3.2. Fluorescent imaging analysis of the Arc-dVenus D1RKD mice

The experimental schedule for electric stimulation and fluorescent image analysis is shown in Fig. 3A. The 3D-reconstituted brain images of Dox (−) Stimulation (+) and Dox (+) Stimulation (+) mice (Fig. 3B, C) demonstrated a clear difference in dVenus signals between the two groups. Reconstituted dVenus signals in layers 1–3 and 5–6 of the cerebral cortex (including the somatosensory, motor, and visual cortices) were stronger in the Dox (−) Stimulation (+) group than those in the Dox (+) Stimulation (+) group. In contrast, reconstituted dVenus signals showed similar intensities between the two groups in the CA1 and CA2 (Fig. 3C).

Volume reconstruction using dVenus signals revealed three areas of observable differences: layers 5–6 of the visual cortex, layers 1–3 of the cerebral cortex (including the somatosensory and motor cortices and excluding the visual cortex) and layers 5–6 of the cerebral cortex (including the somatosensory and motor cortices and excluding the visual cortex) (Fig. 4A–E). Further examination of the differences in layers 5–6 of the visual cortex showed that the Dox (−) Stimulation (−) group had a signal volume that was less than one-third the volume of the Dox (−) Stimulation (+) group ($p < 0.05$) (Fig. 4A). In addition, Dox (+) Stimulation (−) mice showed a slightly lower, but non-significant ($p = 0.21$), dVenus signal volume than that of Dox (+) Stimulation (+) mice (Fig. 4B). Finally, we found that Dox (+) Stimulation (+) mice had a dVenus signal volume less than one-half of that of Dox (−) Stimulation (+) mice ($p < 0.05$) (Fig. 4C).

Comparisons of the dVenus signal volume in layers 1–3 of the cerebral cortex (including the somatosensory and motor cortices and excluding the visual cortex) revealed a lower signal volume (less than one-half) in the D1RKD Dox (+) group compared with that of the Dox (−) group ($p < 0.05$) (Fig. 4D). Furthermore, although Dox-driven differences in layers 5–6 of the cerebral cortex (including the somatosensory and motor cortices and excluding the visual cortex) were smaller than those in layers 1–3, D1RKD Dox (+) mice still exhibited an approximately 50 % lower dVenus signal volume than that of Dox (−) mice ($p < 0.05$) (Fig. 4E). By contrast, the dVenus signal volume in the CA1 and CA2 regions did not significantly differ between Dox administration groups (Fig. 4F). Taken together, these results indicate that Dox inhibition of D1R decreases Arc-controlled dVenus expression in the brain following aversive stimulation.

4. Discussion

Previous evidence from our group has highlighted the importance of D1R-mediated dopaminergic transmission in motor control via its role in phasic activation of the cortical striatal-entopeduncular nucleus direct pathway (Nakamura et al., 2014; Chiken et al., 2015). In addition to this role in motor function, as well as its established role in reward learning (Bjorklund and Dunnett, 2007; Ikemoto, 2010; Nakanishi et al., 2014; Hikida et al., 2016; Schultz, 2019), accumulating evidence suggests that D1R-mediated dopaminergic transmission may also contribute to aversive learning processes (Lammel et al., 2011, 2012; Menegas et al., 2015; Broussard et al., 2016; Menegas et al., 2018; Weele et al., 2019). Thus, here, we expanded on our earlier work to investigate how D1Rs influence aversive memory formation.

In order to investigate the possible role of D1Rs in aversive learning, we generated D1RKD mice in which D1R could conditionally and reversibly be knocked down in response to Dox administration (Chiken et al., 2015). We used these conditional KD mice because D1R-directed dopamine signaling has multiple functions (i.e., as both a mitogen and neurotransmitter) that vary across developmental stages. Therefore, the use of Dox-inducible D1RKD mice allows for the circumventing of any developmental functional

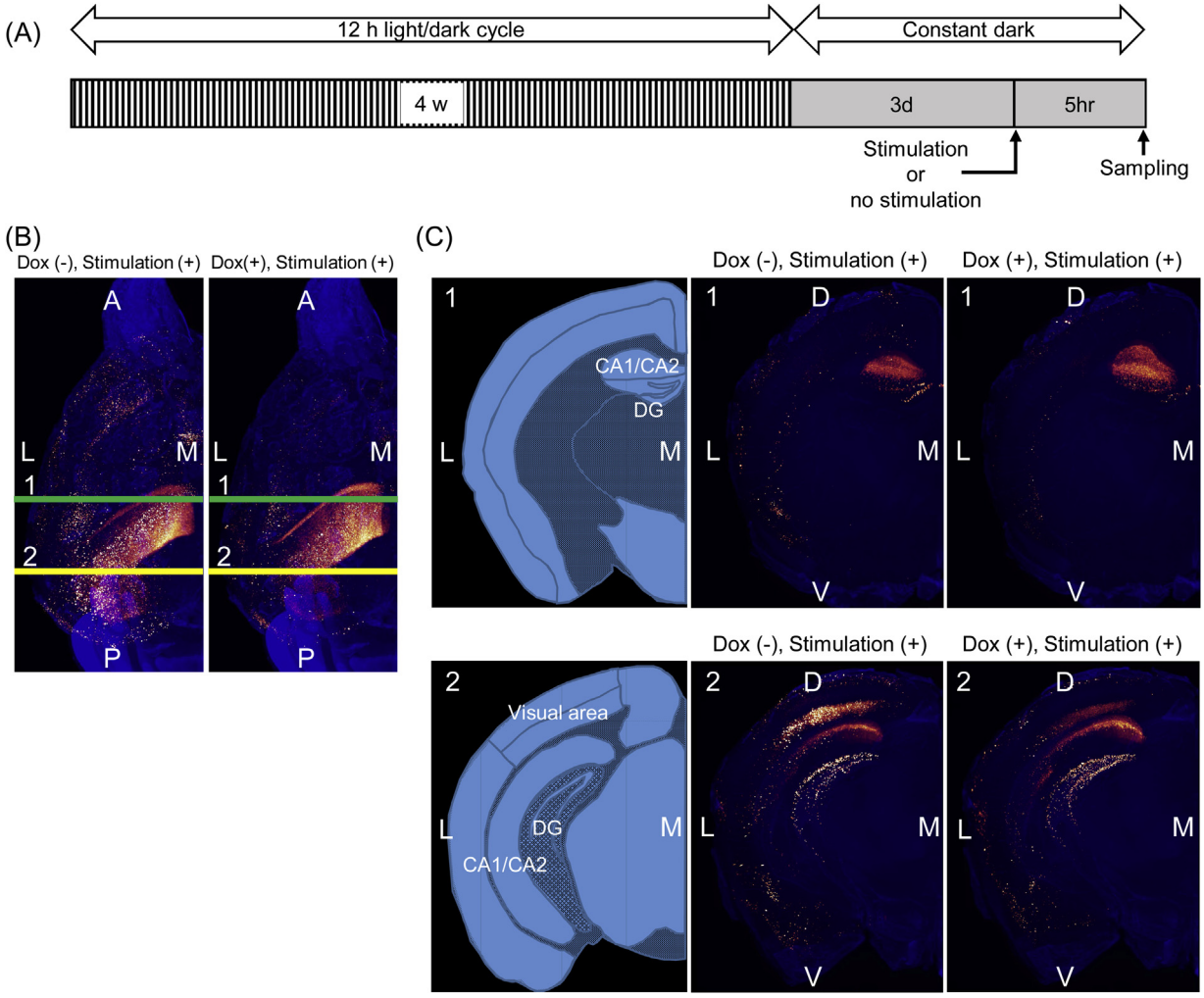

Fig. 3. Three-dimensional (3D)-reconstituted images of Arc-dVenus D1RKD mouse brains using LSF microscopes. Selected images are of the left brain. A, anterior; P, posterior; L, lateral; M, medial; D, dorsal; V, ventral; CA1, hippocampal CA1 region; CA2, hippocampal CA2 region; DG, dentate gyrus. (A) Experimental schedule for stimulation and fluorescent image analysis. D1RKD Dox (+) mice were given Dox (2 mg/mL) in their drinking water for >4 weeks prior to the commencement of the experiment. D1RKD Dox (−) and wild-type (WT) mice were given Dox-free drinking water throughout the entire experiment. Mice in all four groups were maintained under a 12-h light/dark cycle until 3 days before sampling, and were then maintained under constant darkness. The mice were sacrificed for brain removal 5 h post-footshock stimulation. (B) Horizontal views of the 3D-reconstituted whole-brain images of footshock-stimulated Arc-dVenus D1RKD mice. Left panel, dVenus signals of D1RKD Dox(−) mice; right panel, dVenus signals of D1RKD Dox (+) mice. Nuclear staining is in blue. (C) Images of reconstructed coronal sections taken from positions marked 1 (green line) and 2 (yellow line) in whole-brain images from (B). The two figures on the left are maps of respective brain sections.

changes compensating for the loss of D1Rs. Additionally, to analyze neural activity in discrete brain regions, indicated by expression of the IEG Arc, during aversive learning, we crossed D1RKD mice with Arc-dVenus mice. Since these Arc-dVenus mice have remarkably high expression of the reporter gene (nearly 100-fold greater than endogenous *Arc* mRNAs) in the brain, the fluorescence signals can be easily detected. Additionally, the destabilized fluorescent protein, dVenus, of these mice exhibits a rapid decay to basal levels, allowing improved accuracy when determining post-stimulation expression dynamics over other Arc mouse models, including Arc-d2EGFP knockin mice, which have considerably longer fluorescent decay durations that could potentially result in the observation of non-relevant Arc signals (activation prior to the task) (Wang et al., 2006).

Our findings revealed that suppression of D1R expression during memory formation in D1RKD Dox (+) mice resulted in markedly lower performance in the PA test than in D1RKD Dox (−) or WT mice. When D1R expression was recovered in these D1RKD Dox (+) mice, their performance became comparable to that of D1RKD Dox (−) mice. These results suggested that D1R deficiency was responsible for impaired aversive memory formation. However, it is possible that the poor performance observed in D1RKD Dox (+) mice during the PA test may be the result of an impaired ability to sense pain, rather than an impaired ability for in aversive memory formation. Therefore, to examine whether D1RKD Dox (+) mice had a similar ability to sense the electric footshock stimulus, we measured the latency of D1RKD Dox (+) mice to escape to the light compartment after delivery of electrical stimulation in the dark compartment. We observed no significant difference between both D1RKD Dox (+) and D1RKD Dox (−) mice in the latency required to return to the light compartment when compared with WT mice, indicating that D1R suppression did not block the ability to sense pain. However, a potential limitation of the current study is that we did not quantify the degree of pain sensed by animals in each experimental group. As the signal intensity at the time of memory formation may differ depending on the degree of pain felt by the mouse, further investigation of the role of D1Rs in controlling pain sensitivity is required in future studies.

Interestingly, we observed a difference between D1RKD Dox (−) and WT mice in the latency to enter the shock-conditioned dark

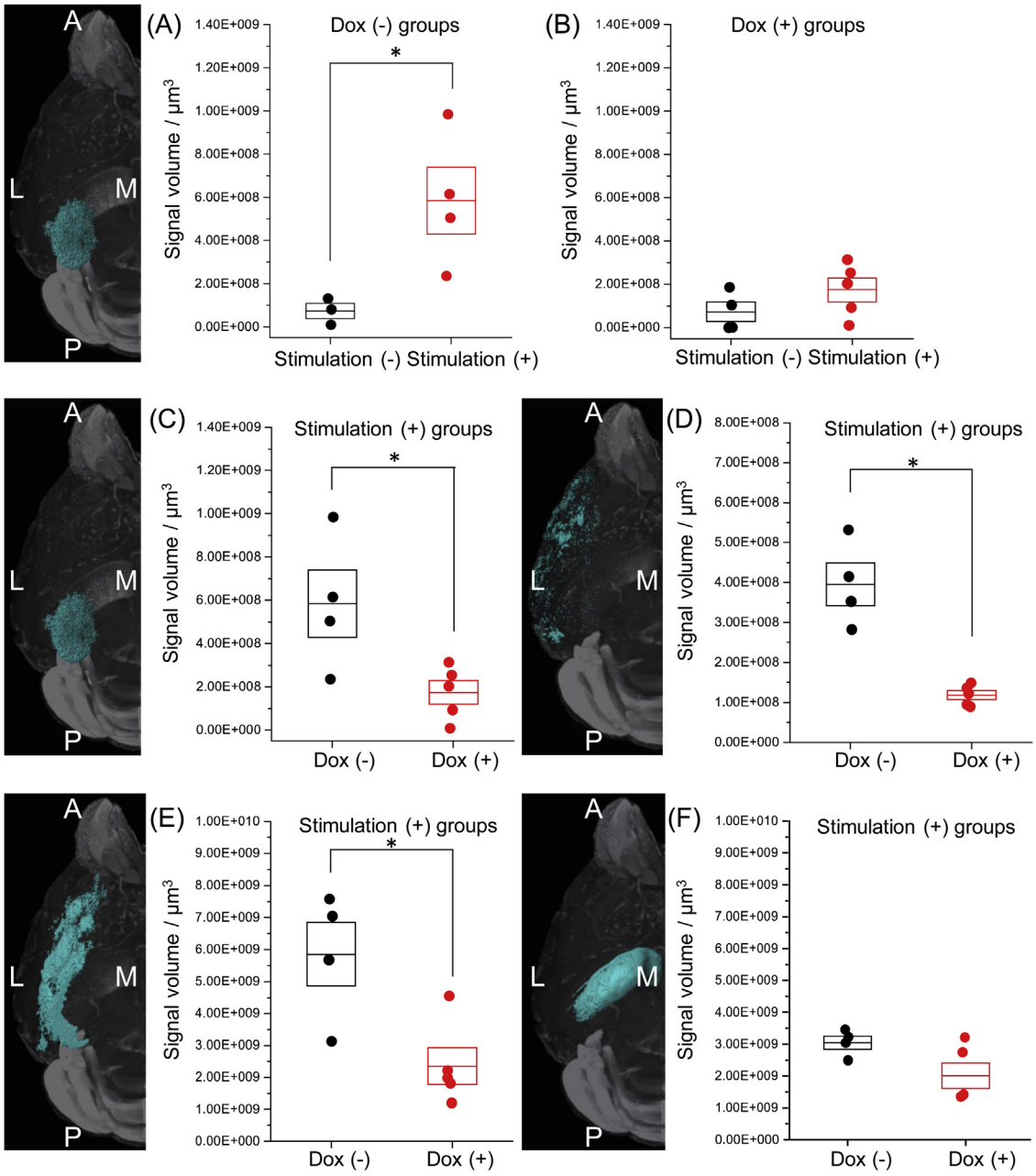

Fig. 4. Analysis of signal volume using Imaris-rendered reconstituted images of Arc-dVenus D1RKD mouse brains (left brain only). *p < 0.05.
(A) Comparison of signal volume in visual cortex layers 5–6 between Stimulation (-) and Stimulation (+) groups without Dox administration. (B) Comparison of signal volume in visual cortex layers 5–6 between Stimulation (-) and Stimulation (+) groups with Dox administration. (C–F) Comparison of signal volume between the D1RKD Dox (-) and D1RKD Dox (+) groups under footshock stimulated conditions. Signal volume measurement areas are shown in blue in the images to the left of the graphs: (A, C) layers 5–6 of the visual cortex; (D) layers 1–3 of the cerebral cortex (including the somatosensory and motor cortices and excluding the visual cortex); (E) layers 5–6 of the cerebral cortex (including the somatosensory and motor cortices and excluding the visual cortex); (F) CA1 and CA2. Black and red dots show the signal volumes of individual samples, and the box plots show means ± SEM. A, anterior; P, posterior; L, lateral; M, medial.

compartment in the later test sessions. Specifically, on days 8 and 15 of the first and second phase test sessions, D1RKD Dox (−) mice showed a shorter latency to enter into the dark compartment than WT mice. While reason for this difference is still unclear, a previous study from our group revealed that D1RKD mice express D1R at a higher level than WT mice during the absence of Dox (Chiken et al., 2015). Further research is needed to determine whether D1R overexpression may contribute to the altered performance of D1RKD Dox (−) mice during the later stages of the PA test.

D1Rs are known to play an important role in the regulation of both hippocamus-dependent plasticity and hipocampus-dependent memory, and are pivotal in conferring the properties of novelty and reward to information being processed by the hippocampus (Hansen and Manahan-Vaughan, 2014). Morevover, recent studies have reported that persistent long-term potentiation via NMDA and D1R-like receptors activation promotes initial memory consolidation within the hippocampus (Takeuchi et al., 2016; Duszkiewicz et al., 2019; Palacios-Filardo and Mellor, 2019). Similarly, D1Rs in the cerebral cortex have repeatedly been implicated in memory-induced long-term plasticity and memory formation and are suggested to control the storage of long-term aversive memories (Puig et al., 2014; Gonzalez et al., 2014). Given the important roles of D1Rs in these regions in learning and memory, we investigated the expression levels of Arc, known to be located downstream

of D1R-mediated neural transmission and suppressed by D1R inactivation, in the hippocampus and cerebral cortex during learning and of an aversive memory (Nishi et al., 2011; Charbonnier-Beaupel et al., 2015). Interestingly, we did not observe any differences between D1RKD Dox (+) and D1RKD Dox (−) groups in CA1 and CA2 Arc expression. However, D1R-suppressed mice exhibited lower expression of Arc in the cortex, including layers 1–3 and 5–6 of the cerebral cortex (including the somatosensory and motor cortices and excluding the visual cortex), and layers 5–6 of the visual cortex compared with D1R-expressing mice, indicating that D1R inhibition led to suppressed Arc expression. As we controlled for the confounding effects of visual stimuli (by performing the experiment in a dark room), these observed patterns could be attributed to the electric footshock.

In conclusion, here, we revealed that D1R-mediated dopaminergic transmission is important for aversive memory formation and that its suppression resulted in a decrease in Arc expression in the cerebral cortex, including the visual, somatosensory, and motor areas, but not the hippocampus. These findings suggest that D1R-mediated dopaminergic transmission may facilitate aversive memory formation at least in part by increasing neural activity within cortical networks. It is still unclear whether D1Rs expressed locally in the cerebral cortex were responsible for the increased neural activity in this area following electric footshock, or whether D1Rs expressed in other brain regions, including the hippocampus, may have indirectly altered cerebral cortex activity. Future investigation using region-specific knockdown of D1Rs may help to clarify this issue. Additionally, future investigation of aversive stimulus-induced expression of other IEGs, such as c-Fos, which are widely expressed in neurons (including within the basal ganglia), will likely prove useful for understanding the neural circuit and molecular mechanism underlying aversive memory formation.

Author contributions

N.S. and T.S. designed the research; N.S. and K.T. performed the research and N.S., K.T., T.M., T.H. and T.S. analyzed the data; S.Y. provided the genetically modified mice; N.S., T.M., T.H. and T.S. wrote the paper.

Funding

This work was supported by a Grant-in-Aid for Scientific Research from the Japan Society for the Promotion of Science [grant number 26290029, 18H02540, T.S.]; a Grant-in-Aid for Scientific Research on Innovative Areas (Non-linear Neuro-oscillology: Towards Integrative Understanding of Human Nature from the Ministry of Education, Culture, Sports, Science and Technology, Japan [grant number 16H01606, 18H04937; T.S.]; and the Cooperative Study Program [grant number 228, 19-201: T.S.] of the National Institute for Physiological Sciences.

Declaration of Competing Interest

None.

Acknowledgments

We thank the members of Department of Comparative and Experimental Medicine in the Brain Research Institute at Niigata University for their assistance and discussion and Drs. Keisuke Yonehara of Aahus University and Hironaka Igarashi of Brain Research Institute Niigata University for their critical reading and comments.

Appendix A. Supplementary data

Supplementary material related to this article can be found, in the online version, at doi:https://doi.org/10.1016/j.neures.2020.04.006.

References

Bjorklund, A., Dunnett, S.B., 2007. Dopamine neuron systems in the brain: an update. Trends Neurosci. 30, 194–202.
Broussard, J.I., Yang, K., Levine, A.T., Tsetsenis, T., Jenson, D., Cao, F., Garcia, I., Arenkiel, B.R., Zhou, F.M., De Biasi, M., Dani, J.A., 2016. Dopamine regulates aversive contextual learning and associated in vivo synaptic plasticity in the hippocampus. Cell Rep. 14, 1930–1939.
Charbonnier-Beaupel, F., Malerbi, M., Alcacer, C., Tahiri, K., Carpentier, W., Wang, C., During, M., Xu, D., Worley, P.F., Girault, J.A., Herve, D., Corvol, J.C., 2015. Gene expression analyses identify Narp contribution in the development of L-DOPA-induced dyskinesia. J. Neurosci. 35, 96–111.
Chiken, S., Sato, A., Ohta, C., Kurokawa, M., Arai, S., Maeshima, J., Sunayama-Morita, T., Sasaoka, T., Nambu, A., 2015. Dopamine D1 receptor-mediated transmission maintains information flow through the cortico-striato-entopeduncular direct pathway to release movements. Cereb. Cortex 25, 4885–4897.
Chowdhury, S., Shepherd, J.D., Okuno, H., Lyford, G., Petralia, R.S., Plath, N., Kuhl, D., Huganir, R.L., Worley, P.F., 2006. Arc/Arg3.1 interacts with the endocytic machinery to regulate AMPA receptor trafficking. Neuron 52, 445–459.
Duszkiewicz, A.J., McNamara, C.G., Takeuchi, T., Genzel, L., 2019. Novelty and dopaminergic modulation of memory persistence: a tale of two systems. Trends Neurosci. 42, 102–114.
Eguchi, M., Yamaguchi, S., 2009. In vivo and in vitro visualization of gene expression dynamics over extensive areas of the brain. Neuroimage 44, 1274–1283.
Gonzalez, M.C., Kramer, C.P., Tomaiuolo, M., Katche, C., Weisstaub, N., Cammarota, M., Medina, J.H., 2014. Medial prefrontal cortex dopamine controls the persistent storage of aversive memories. Front. Behav. Neurosci. 8 (408), 1–7.
Granado, N., Ortiz, O., Suarez, L.M., Martin, E.D., Cena, V., Solis, J.M., Moratalla, R., 2008. D1 but not D5 dopamine receptors are critical for LTP, spatial learning, and LTP-Induced arc and zif268 expression in the hippocampus. Cereb. Cortex 18, 1–12.
Hansen, N., Manahan-Vaughan, D., 2014. Dopamine D1/D5 receptors mediate informational saliency that promotes persistent hippocampal long-term plasticity. Cereb. Cortex 24, 845–858.
Hikida, T., Morita, M., Macpherson, T., 2016. Neural mechanisms of the nucleus accumbens circuit in reward and aversive learning. Neurosci. Res. 108, 1–5.
Ikemoto, S., 2010. Brain reward circuitry beyond the mesolimbic dopamine system: a neurobiological theory. Neurosci. Biobehav. Rev. 35, 129–150.
Lammel, S., Ion, D.I., Roeper, J., Malenka, R.C., 2011. Projection-specific modulation of dopamine neuron synapses by aversive and rewarding stimuli. Neuron 70, 855–862.
Lammel, S., Lim, B.K., Ran, C., Huang, K.W., Betley, M.J., Tye, K.M., Deisseroth, K., Malenka, R.C., 2012. Input-specific control of reward and aversion in the ventral tegmental area. Nature 491, 212–217.
Mastwal, S., Cao, V., Wang, K.H., 2016. Genetic feedback regulation of frontal cortical neuronal ensembles through activity-dependent arc expression and dopaminergic input. Front. Neural Circuits 10, 100.
Menegas, W., Bergan, J.F., Ogawa, S.K., Isogai, Y., Umadevi Venkataraju, K., Osten, P., Uchida, N., Watabe-Uchida, M., 2015. Dopamine neurons projecting to the posterior striatum form an anatomically distinct subclass. Elife 4, e10032.
Menegas, W., Akiti, K., Amo, R., Uchida, N., Watabe-Uchida, M., 2018. Dopamine neurons projecting to the posterior striatum reinforce avoidance of threatening stimuli. Nat. Neurosci. 21, 1421–1430.
Nakamura, T., Sato, A., Kitsukawa, T., Momiyama, T., Yamamori, T., Sasaoka, T., 2014. Distinct motor impairments of dopamine D1 and D2 receptor knockout mice revealed by three types of motor behavior. Front. Integr. Neurosci. 8, 56.
Nakanishi, S., Hikida, T., Yawata, S., 2014. Distinct dopaminergic control of the direct and indirect pathways in reward-based and avoidance learning behaviors. Neuroscience 282, 49–59.
Nishi, A., Kuroiwa, M., Shuto, T., 2011. Mechanisms for the modulation of dopamine d(1) receptor signaling in striatal neurons. Front. Neuroanat. 5, 43.
Okubo, T., Sato, A., Okamoto, H., Sato, T., Sasaoka, T., 2018. Differential behavioral phenotypes of dopamine D1 receptor knockdown mice at the embryonic, postnatal, and adult stages. Int. J. Dev. Neurosci. 66, 1–8.
Okuno, H., Minatohara, K., Bito, H., 2018. Inverse synaptic tagging: an inactive synapse-specific mechanism to capture activity-induced Arc/arg3.1 and to locally regulate spatial distribution of synaptic weights. Semin. Cell Dev. Biol. 77, 43–50.
Palacios-Filardo, J., Mellor, J.R., 2019. Neuromodulation of hippocampal long-term synaptic plasticity. Curr. Opin. Neurobiol. 54, 37–43.
Puig, V.M., Rose, J., Schmidt, R., Freund, N., 2014. Dopamine modulation of learning and memory in the prefrontal cortex: insights from studies in primates, rodents, and birds. Front. Neural Circuits 8 (93), 1–15.
Renier, N., Adams, E.L., Kirst, C., Wu, Z., Azevedo, R., Kohl, J., Autry, A.E., Kadiri, L., Umadevi Venkataraju, K., Zhou, Y., Wang, V.X., Tang, C.Y., Olsen, O., Dulac, C., Osten, P., Tessier-Lavigne, M., 2016. Mapping of brain activity by automated volume analysis of immediate early genes. Cell 165, 1789–1802.

Schultz, W., 2019. Recent advances in understanding the role of phasic dopamine activity. F1000Research.

Susaki, E.A., Tainaka, K., Perrin, D., Kishino, F., Tawara, T., Watanabe, T.M., Yokoyama, C., Onoe, H., Eguchi, M., Yamaguchi, S., Abe, T., Kiyonari, H., Shimizu, Y., Miyawaki, A., Yokota, H., Ueda, H.R., 2014. Whole-brain imaging with single-cell resolution using chemical cocktails and computational analysis. Cell 157, 726–739.

Tainaka, K., Murakami, T.C., Susaki, E.A., Shimizu, C., Saito, R., Takahashi, K., Hayashi-Takagi, A., Sekiya, H., Arima, Y., Nojima, S., Ikemura, M., Ushiku, T., Shimizu, Y., Murakami, M., Tanaka, K.F., Iino, M., Kasai, H., Sasaoka, T., Kobayashi, K., Miyazono, K., Morii, E., Isa, T., Fukayama, M., Kakita, A., Ueda, H.R., 2018. Chemical landscape for tissue clearing based on hydrophilic reagents. Cell Rep. 24, 2196–2210, e2199.

Takeuchi, T., Duszkiewicz, A.J., Sonneborn, A., Spooner, P.A., Yamasaki, M., Watanabe, M., Smith, C.C., Fernandez, G., Deisseroth, K., Greene, R.W., Morris, R.G., 2016. Locus coeruleus and dopaminergic consolidation of everyday memory. Nature 537, 357–362.

Vazdarjanova, A., Ramirez-Amaya, V., Insel, N., Plummer, T.K., Rosi, S., Chowdhury, S., Mikhael, D., Worley, P.F., Guzowski, J.F., Barnes, C.A., 2006. Spatial exploration induces ARC, a plasticity-related immediate-early gene, only in calcium/calmodulin-dependent protein kinase II-positive principal excitatory and inhibitory neurons of the rat forebrain. J. Comp. Neurol. 498, 317–329.

Wang, K.H., Majewska, A., Schummers, J., Farley, B., Hu, C., Sur, M., Tonegawa, S., 2006. In vivo two-photon imaging reveals a role of arc in enhancing orientation specificity in visual cortex. Cell 126, 389–402.

Weele, C.M.V., Siciliano, C.A., Tye, K.M., 2019. Dopamine tunes prefrontal outputs to orchestrate aversive processing. Brain Res. 1713, 16–31.

Zhang, W., Wu, J., Ward, M.D., Yang, S., Chuang, Y.A., Xiao, M., Li, R., Leahy, D.J., Worley, P.F., 2015. Structural basis of arc binding to synaptic proteins: implications for cognitive disease. Neuron 86, 490–500.